

# Characterization of Water Structure in Cellulose Acetate Membranes by Calorimetric Measurements

H.-G. BURGHOFF and W. PUSCH, *Max-Planck-Institut für Biophysik, Frankfurt am Main, Germany*

## Synopsis

The heat capacities of homogeneous and asymmetric cellulose acetate membranes have been measured at different water contents within the temperature range of  $-40$  to  $+20^{\circ}\text{C}$ . The experimental heat capacity-temperature curves were verified by DTA measurements within a temperature range of  $-120$  to  $+20^{\circ}\text{C}$ . The results for the partial heat capacity of water within the membranes as well as for the heat of fusion were interpreted by assuming two different states of water—unfreezing bound water due to a sorption process and unbound water due to capillary phenomena, which freezes with a freezing point depression and a reduced heat of fusion.

## INTRODUCTION

During the late fifties, Reid and Breton<sup>1</sup> proved homogeneous cellulose acetate (CA) membranes to be nearly impermeable to salts but highly permeable to water. Parallel to these investigations, Loeb and Sourirajan<sup>2</sup> developed the so-called "asymmetric" CA membranes possessing the same high salt rejection as the homogeneous CA membranes but a higher water permeability.

The extraordinary high water permeability generated a great deal of interest in the structure of these membranes. Under the electron microscope, the asymmetric membranes appeared to consist of an extremely thin but also extremely dense layer on the air-dried surface and a very porous matrix.<sup>3,4</sup> The thickness of the dense or "active" layer was estimated to be in the range of  $0.05$  to  $0.3\ \mu\text{m}$ . The overall membrane thickness is typically in the order of  $100\ \mu\text{m}$ . The pores in the matrix were estimated to be in the order of  $0.1\ \mu\text{m}$  in diameter. Earlier electron microscopy (EM) studies<sup>3,4</sup> revealed no pore structures either in homogeneous CA membranes or in the dense layer of asymmetric CA membranes.

However, more recent EM studies<sup>25-27</sup> suggest the presence of pores within the dense or active layer of asymmetric CA membranes as do gas permeation measurements performed by Stern et al.<sup>5</sup> Stern et al. estimated the pore diameters to be in the range of  $1 \times 10^{-8}$  to  $50 \times 10^{-8}$  cm. Recent work assumes micropores of the same dimensions to exist throughout a homogeneous CA membrane and on that basis interprets some data from previous water sorption experiments.<sup>6</sup> In addition, the states of salt and water in homogeneous and asymmetric membranes were investigated since transport properties of membranes are clearly related to the physical state of the transported species within a membrane.

Extensive studies on sorption and diffusion of water in CA membranes have been performed.<sup>6-9</sup> The results of these investigations were interpreted applying

various models such as the Flory-Huggins equation, the Zimm-Lundberg description, and the BET model. Each of these models yields a different description of the state of water within the CA membranes. Multiphase phenomena such as capillary condensation within the pores of the supporting substructure have also been used to interpret the rapid increase of dissolved water in asymmetric membranes at relative humidities above 70%. Assuming validity of the Kelvin equation, Lonsdale et al.<sup>7</sup> as well as Burghoff and Pusch<sup>6</sup> estimated consistent distributions of pore radii within the porous matrix of asymmetric membranes to be bounded by 0.01 and 0.5  $\mu\text{m}$ .

Calorimetry has been proved to be an additional sensitive technique for investigating the state of adsorbed water. Taniguchi and Horigome<sup>10</sup> studied melting endotherms of water in CA membranes by differential scanning calorimetry. They detected no phase transition at all in homogeneous membranes. With asymmetric membranes, phase transitions appeared only at water contents higher than 13 wt-% within a temperature range of  $-15$  to  $0^\circ\text{C}$ . In addition, melting peaks were found at water contents above 18 wt-% which were due to the melting of ice. Yasuda et al.<sup>11</sup> specifically measured the heat of fusion in water-glycerol monomethacrylate systems and found no phase transition at water contents up to 0.36 g  $\text{H}_2\text{O}/\text{g}$  dry polymer. It was thus assumed that up to this water content the water present is so-called bound water only, whereas water being sorbed in excess of 0.36 g is supposed to be free water crystallizing with normal heat of fusion. Plooster and Gittlin<sup>12</sup> reported results similar to these of Taniguchi and Horigome for the state of water adsorbed on silica surfaces. They estimated the heat of melting of ice at temperatures less than  $0^\circ\text{C}$  to be smaller than the heat of melting of normal ice. Only limited data of heat capacity and heat of phase transition are available in the literature for water in CA membranes.

It is the purpose of this paper, therefore, to present data of systematic calorimetric studies of heat capacity, melting point, and heat of melting of dissolved water in both homogeneous and asymmetric membranes. These data are interpreted by considering results of sorption measurements and the thermodynamics of capillary condensation.

## EXPERIMENTAL

Homogeneous membranes were cast from chloroform solutions of cellulose acetate (39.1 wt-% acetyl; Cellit K 700 of the Bayer Company, Leverkusen, Germany) using a casting solution with 10 wt-% Cellit. The final thickness of the dried membranes was about 30  $\mu\text{m}$ . In addition, asymmetric cellulose acetate membranes were cast from a ternary casting solution of Cellit K 700 in an acetone-formamide mixture according to the procedure of Manjikian, Loeb, and McCutchan.<sup>13</sup> The overall thickness of these asymmetric membranes was about 100  $\mu\text{m}$ . The nonannealed asymmetric membranes were soaked in water at  $25^\circ\text{C}$  for one week. Thereafter, the homogeneous and conditioned asymmetric CA membranes were contacted with air of various humidities in an air-conditioning system at  $35^\circ\text{C}$ . The humidities and temperature were maintained constant within  $\pm 0.8\%$  and  $\pm 0.2^\circ\text{C}$ , respectively. The water content of the membranes is well known from water sorption isotherms reported previously<sup>6</sup> and reproduced in Figure 1. For each calorimetric run, membrane samples of about 0.5 g each were used. Monitoring the weights of the membrane samples before and after every calorimetric run indicated no weight change during an experiment.

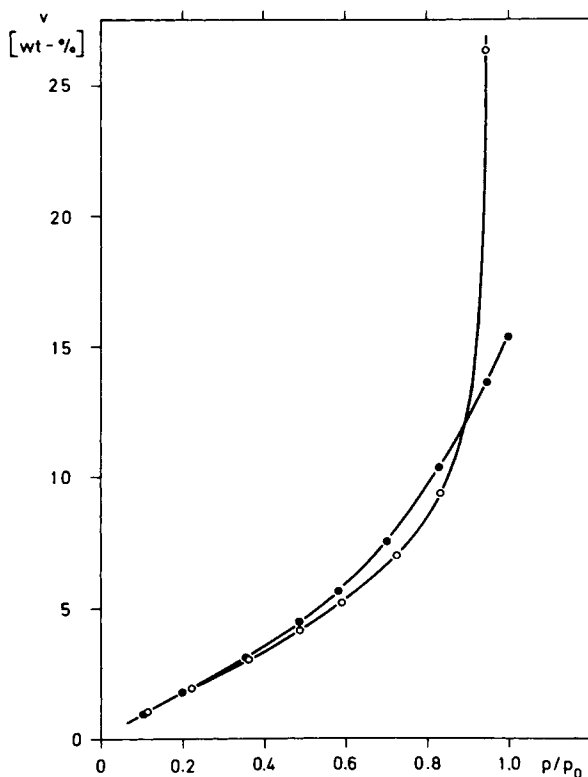


Fig. 1. Desorption isotherms of a homogeneous (●) and an unannealed asymmetric (○) cellulose acetate membrane at 35°C. Regain  $v$  in wt % referred to dry membrane material.<sup>6,13</sup>

The adiabatically isolated continuous heating-type calorimeter was a thin-walled stainless steel cylinder 8 mm in diameter and 25 mm high, sealed with a plastic hood. The heating element, a 100-ohm platinum resistor 4 mm in diameter and 25 mm high was placed in the center of the cylinder. This calorimeter unit itself was fixed in the center of a cylindrical adiabatic shield made from stainless steel. The shield was taped by a suitable resistance wire. The temperature of the shield was controlled by a two-valued response regulator using the amplified emf difference of two Chromel–Alumel thermocouples, one of which contacts the outside wall of the sample container and the second one contacts the inside wall of the adiabatic shield. The heating voltage of the heater was chosen such that the emf difference of the two thermocouples oscillated symmetrically around zero. The adiabatic shield, serving also as the calorimeter vessel, was evacuated. The entire assembly was then mounted in a Dewar flask and cooled down overnight by means of liquid nitrogen before each experimental run. Thus prepared, the calorimeter containing the membrane sample was heated by means of a constant-current source, the temperature of the calorimeter being measured with a Chromel–Alumel thermocouple referred to an ice bath. A Hewlett-Packard 9821 A calculator was used to trigger a digital voltmeter and to read, on-line, the emf of the thermocouple and the heating voltage at regular time intervals. With these data the HP 9821 A calculated and plotted the heat capacity of the whole assembly (calorimeter and its contents) as a function of temperature.

The heat capacity of the empty calorimeter was determined to be 0.97 J/degree

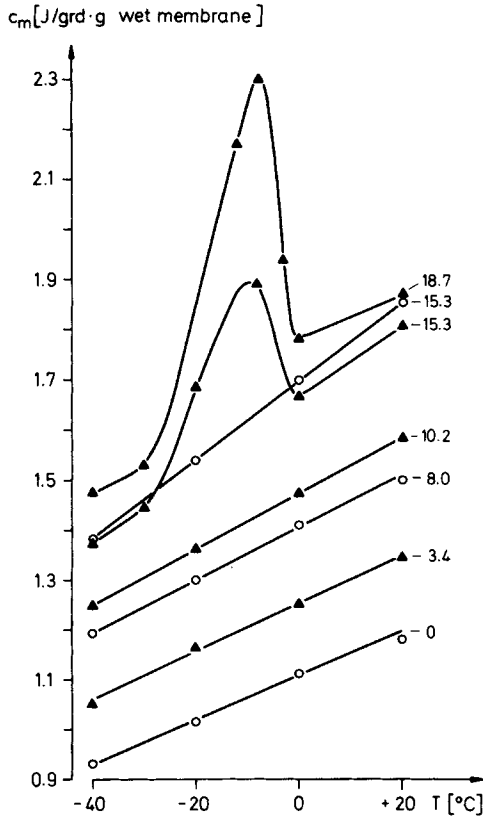


Fig. 2. Heat capacity of a homogeneous (O) and an unannealed asymmetric (▲) cellulose acetate membrane as function of temperature at various water contents. The water content of a sample is given in wt % referred to dry membrane material.

at  $-40^{\circ}\text{C}$  and  $0.99\text{ J/degree}$  at  $20^{\circ}\text{C}$ . This temperature dependence of the heat capacity is mainly due to that of stainless steel. Test runs with 100 and 300 mg water over a temperature range of  $-40^{\circ}\text{C}$  to  $+25^{\circ}\text{C}$  yielded results for the heat capacity, the heat of melting, and the melting point of ice in excellent agreement with well-known data from the literature.<sup>14</sup> The accuracy of the measured heat capacity of water was  $0.01\text{ J/degree}\cdot\text{g}$ . This error was caused by uncontrolled heat flows. The heat content of the samples ranged from 0.7 to 1.8 J/degree. Therefore, the error of the measured heat capacity was always less than 3%. The reproducibility of the measured heat capacity in repeated runs with a given sample was better than 1%. Temperatures were accurate to within  $0.25^{\circ}\text{C}$ , caused by amplifier drifts.

## RESULTS AND ANALYSIS

Measured heat capacities  $c_m$  of homogeneous and asymmetric CA membranes at various water contents as functions of temperature are presented in Figure

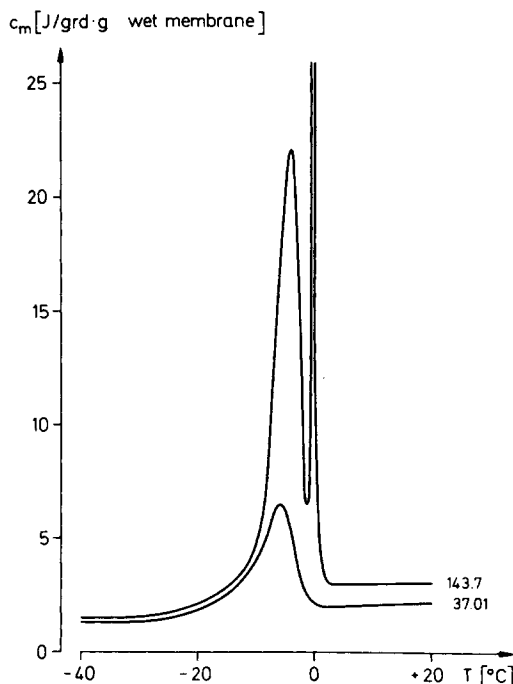


Fig. 3. Heat capacity of an unannealed asymmetric cellulose acetate membrane as function of temperature at high water contents. The water content of a sample is given in wt-% referred to dry membrane material.

2.\* The water content  $v$  of a membrane is given in wt-% referred to the dry membrane material. With homogeneous CA membranes the heat capacity increases monotonically with temperature, with no detectable peaks. For a given water content of less than about 15 wt-%, no difference was observed between the heat capacity of a homogeneous and an asymmetric membrane. On the other hand, at a water content somewhat above 15 wt-% in an asymmetric membrane, a broad maximum in the heat capacity-temperature curves appeared within the temperature range of  $-30$  to  $-1^{\circ}\text{C}$ , peaking at  $-9^{\circ}\text{C}$ . At higher water contents the peak temperature increased continuously with increasing water content but never approached  $0^{\circ}\text{C}$ . A second very sharp peak appeared at  $0^{\circ}\text{C}$  within the heat capacity-temperature curves of asymmetric CA membranes at near saturation water contents. This sharp peak at  $0^{\circ}\text{C}$  corresponds to a first-order phase transition of bulk water. The corresponding heat capacity-temperature curves are represented in Figure 3. [The heat capacity-temperature curves shown in Figs. 2 and 3 were verified by DTA control measurements within a temperature range of  $-120$  to  $20^{\circ}\text{C}$  (DTA type L62, manufactured by Linseis, Selb, Germany).

\* The heat capacity  $c_m$  is measured at constant pressure (atmospheric pressure). The difference

$$c_p - c_v = \alpha TV/k$$

where  $c_v$  is the heat capacity at constant volume,  $T$  is the temperature in K,  $V$  is the volume of the system,  $\alpha$  is the thermal expansion coefficient, and  $k$  is the isothermal compressibility, is less than 2% of the value of  $c_p$  for CA membranes. Therefore, no difference is made between  $c_p$  and  $c_v$  in the following discussion.

The shapes of the heat capacity–temperature curves presented in Figs. 2 and 3 are quite consistent with the melting endotherms reported by Taniguchi and Horigome.<sup>10]</sup>

The origin of this additional peak in the heat capacity–temperature curves of asymmetric membranes can be clarified by taking into account that the peak at 0°C coincides with the appearance of water on the surface of the asymmetric membranes after a calorimetric run. However, no water was ever detected visually before starting a calorimetric run. This important observation might be a consequence of the experimental procedure. If the samples are cooled down to –150°C at the beginning of an experiment, some of the water dissolved in an asymmetric membrane will be frozen. At a water content near saturation, a part of the frozen water is driven out of the membrane by freeze drying. This water on the macroscopic surface of the membrane cannot return into the pores during the gradual heating. Therefore, this frozen water melts at 0°C like bulk water and thus creates the corresponding peak in the heat capacity–temperature curves of asymmetric CA membranes. Obviously, this water does not represent an independent state of water within the membrane. This interpretation is contrary to that of Taniguchi and Horigome,<sup>10</sup> who suggested that the melting peak at 0°C corresponds to completely free water in an asymmetric membrane.

As the melting peak of the phase transition at 0°C was extremely sharp, the amount of ice melting could be calculated easily from the quantity of heat added to the calorimeter, assuming the specific heat of melting to be the same as for bulk water, 333.7 J/g. In Figure 4 the amount of ice  $v_i$  melting at 0°C is presented as a function of the total water content  $v$  of an asymmetric membrane. The experimental data fit a straight line with slope 1 and an intercept with the abscissa of 92 wt-%.

To determine the heat of phase transition in the temperature range of diffused melting below 0°C, the heat capacity of a sample within the transition region has to be known. Clearly, this heat capacity cannot be determined directly by measurement because of the superposed melting energy of ice. However, one might obtain a calculated heat capacity of a sample by knowledge of the partial quantities of heat capacity and masses of both water and membrane material

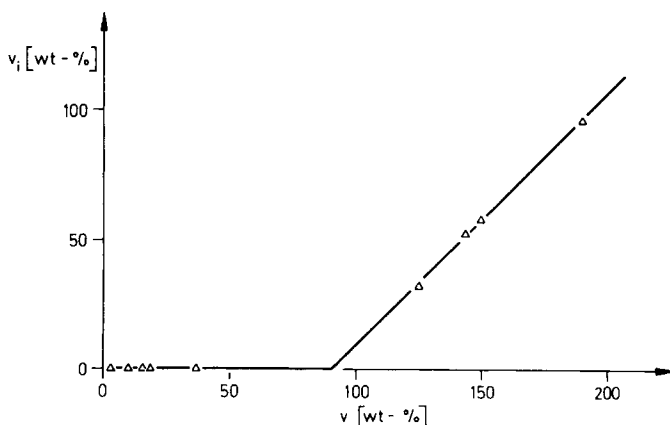


Fig. 4. Amount of ice  $v_i$  melting at 0°C as function of total water content  $v$  of asymmetric membranes.  $v_i$  and  $v$  are given in wt % referred to dry membrane material.

within the sample. Therefore, the experimental results will be used to derive these partial heats by the following analysis.

The partial heat capacities of both water  $\bar{c}_w$ , and CA membrane material,  $\bar{c}_c$ , can be calculated from the measured heat capacity  $c_m$  of a water-containing membrane sample by using the following relationship:

$$c_m = \frac{w_w \bar{c}_w + w_c \bar{c}_c}{w_w + w_c} \quad (1)$$

where  $w_w$  and  $w_c$  are the weights of water and membrane, respectively.<sup>15,16</sup> Choosing  $w_c$  to be 1 g,  $w_w$  corresponds to the water content of the membrane in grams water per gram dry membrane,  $v^* = v/100$ . Thus, eq. (1) might be rewritten to yield

$$(v^* + 1)c_m = \bar{c}_c + \bar{c}_w v^* \quad (2)$$

The slope of a tangent at any point of the curve  $(v^* + 1)c_m$  versus  $v^*$  corresponds to  $\bar{c}_w$  and its intercept with the ordinate to  $\bar{c}_c$ . Such plots of the experimental values at 20°C are presented in Figure 5(a) for homogeneous and asymmetric CA membranes at water contents less than 16 wt-% and in Figure 5(b) for asymmetric CA membranes at water contents up to saturation. Plots of experimental data obtained at other temperatures between -40 and 20°C have a similar linearity.

While the heat capacity data obtained with homogeneous CA membranes fit eq. (2) quite well up to a water content of saturation, a straight line with the same slope is obtained for asymmetric CA membranes only up to a water content of 16 wt-% at all temperatures. From 16 wt-% up to saturation water content, a new straight-line relationship resumes, as can be seen from Figure 5(b), indicating an abrupt change in the partial heat capacity of water in the asymmetric CA membrane at a water content of 16 wt-%. The smaller slope of this second straight line yields a partial heat capacity of the extra water in asymmetric membranes, essentially identical with either the heat capacity of ice or bulk water depending on the temperature. On the other hand, it is obvious that  $\bar{c}_w$  and  $\bar{c}_c$  are each identical for the two types of CA membranes below 16 wt-% water content. In addition, it might be concluded that the partial heat capacities,  $\bar{c}_w$  and  $\bar{c}_c$ , are independent of the water content for both membranes below a water content of 16 wt-%.

No distinction can also be made between homogeneous and asymmetric CA membranes with respect to the temperature dependence of the partial heat capacities of water and membrane materials at water contents less than 16 wt-%. As can be seen from Figure 6, where the heat capacities of ice, bulk water, and saturated vapor are drawn in for comparison, the partial heat capacity of dissolved water is always larger than that of ice or liquid water at the same temperature. Furthermore, the partial heat capacity of the membrane materials is directly proportional to the temperature. A similar relationship has also been proved to exist for wool by Haly and Snaith.<sup>19</sup> As shown by Tarasov,<sup>20</sup> this linear relationship results from a theoretical treatment using the one-dimensional Debye term for the vibrations of the polymer chains.

To determine the heat of fusion at temperatures below 0°C from the experimental  $c_m$  data, a calculated heat capacity of a sample within the temperature

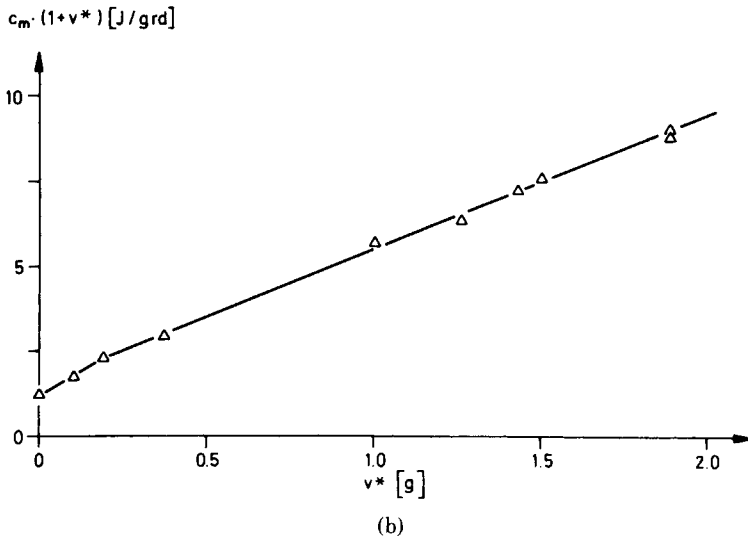
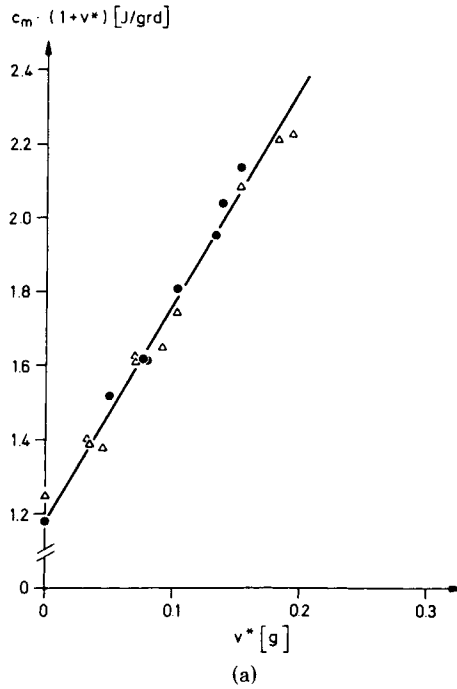


Fig. 5. (a) Plot of  $(1 + v^*)c_m$  as function of  $v^*$  at 20°C for a homogeneous (●) and an unannealed asymmetric (Δ) cellulose acetate membrane at water contents less than 20 wt-%. (b) Plot of  $(1 + v^*)c_m$  as function of  $v^*$  at 20°C for an unannealed asymmetric cellulose acetate membrane at water contents up to saturation.



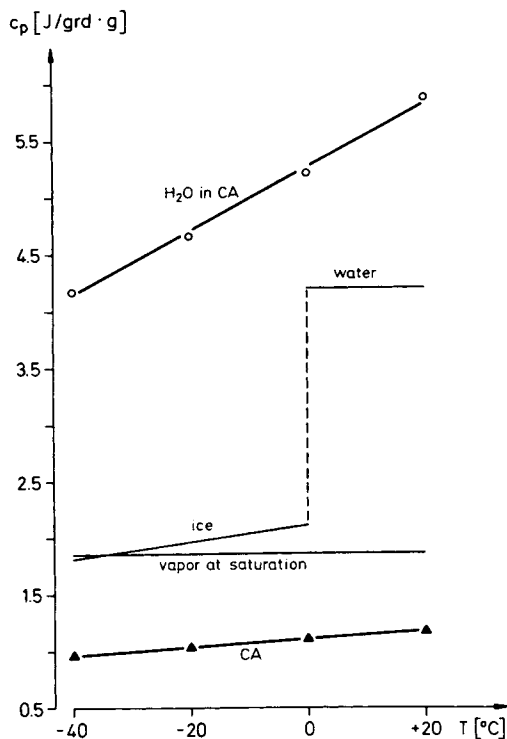


Fig. 6. Calculated partial heat capacities of a cellulose acetate membrane ( $\blacktriangle$ ) and sorbed water ( $\circ$ ) as function of temperature. In addition, heat capacities of ice, bulk water, and saturated vapor are presented for comparison.

range of  $-30$  to  $0^\circ\text{C}$  may be obtained with respect to the here presented results by use of the following assumptions: (a) The amount of water in an asymmetric membrane possessing a higher partial heat capacity compared to bulk water is equal to the amount of water of a homogeneous membrane,  $v$ , and thus its water content at the corresponding water activity. (b) The amount of ice melting in an asymmetric membrane at temperatures below  $0^\circ\text{C}$  is given by the difference between the total amount of water and the amount of surface water melting at  $0^\circ\text{C}$  plus the amount of water possessing the higher partial heat capacity.

The overall heat capacity of a 1-g sample might be considered as linear combination of the partial quantities describing membrane material and the two states of dissolved water. The heat of fusion at temperatures below  $0^\circ\text{C}$  is given by the difference between the total heat added to the system within the temperature range of  $-30$  to  $0^\circ\text{C}$  and the energy necessary to heat up the system from  $-30$  to  $0^\circ\text{C}$  calculated by means of the overall heat capacity of the sample. The result is shown in Figure 7. The heat of melting,  $\Delta H_s$ , is plotted as a function of the amount of ice melting at temperatures below  $0^\circ\text{C}$ . The linear relationship obtained suggests that the specific heat of fusion is independent of the amount of melted ice. The slope of the curve yields a specific heat of fusion of  $231$  J/g.

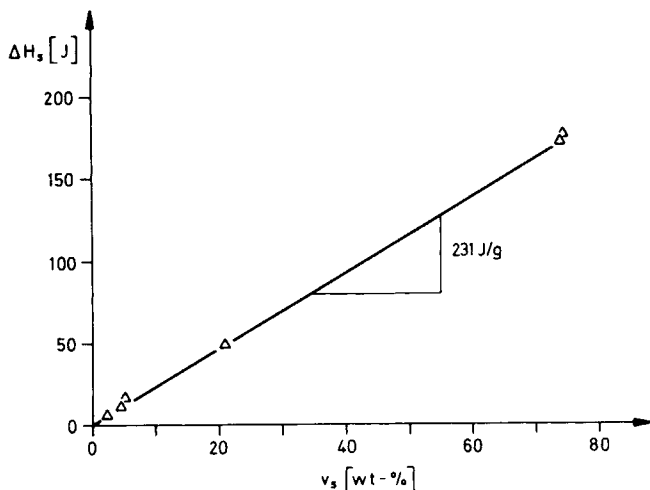


Fig. 7. Heat of fusion  $\Delta H_s$  of ice melting in asymmetric cellulose acetate membranes at temperatures below  $0^\circ\text{C}$  as function of the amount of melting ice  $v_s$ .

## DISCUSSION

The larger heat capacity of sorbed water at low water contents of the membranes may be explained by introducing a simple model. The heat of sorption connected to the sorption of water by CA membranes indicates a strong interaction between the sorbed water molecules and the polymer chain, such as the formation of hydrogen bonds. In general, the sorption energy results in an excess heat capacity over the heat capacity of bulk water. This model together with the experimental findings leads to the conclusion that all the water sorbed by homogeneous CA membranes is purely dissolved as bound water. The same conclusion is valid for the sorbed water in asymmetric CA membranes at water contents lower than 16 wt-%. This conclusion is consistent with the experimentally established fact that no real difference exists in the water uptake between a homogeneous and an asymmetric CA membrane at lower water contents. Since the heat capacity  $\bar{c}_c$  of CA membranes is independent of the water content, the membrane structure should be essentially unchanged by adsorption of water molecules, unlike the solvation process which would take place in homogeneous and asymmetric membranes in the presence of strong organic solutes such as phenol.<sup>17,18</sup> The fact that the smaller partial heat capacity of water observed with asymmetric CA membranes at larger water contents equals the heat capacity of bulk water indicates nearly no interaction of the additional water with the polymer backbone. Furthermore, the decrease in the partial heat capacity of water coincides with the onset of rapid increase in water content in these asymmetric membranes as a function of regain. Since it is well known that this strong increase in water content is due to capillary condensation of water in the porous substructure of the asymmetric membranes, the present heat capacity observation supports the idea of well-defined pores existing in the matrix of asymmetric membranes.<sup>6,7</sup> The additional water sorbed by capillary condensation can thus be assumed to be a second state of water within asymmetric membranes.

The correlation of the decrease in heat capacity to capillary condensation is quite consistent with the coinciding phase transition phenomena below  $0^\circ\text{C}$  since

the thermodynamic treatment of capillary phenomena predicts melting point depression and a reduced heat of fusion for water condensed in small pores, whereas the heat capacity of pore water is quite similar to that of bulk water.<sup>22-24</sup> It may therefore be suggested that the broad maxima in the heat capacity-temperature curves of asymmetric membranes are due to first-order transitions of water in nonuniform-sized pores.

As Kuhn<sup>23</sup> has shown, the melting temperature  $T_s$  of a microcrystal is related to its size by

$$T_s - T_0 = -4\sigma_k v_k T_0 / d \Delta H_s \quad (3)$$

where  $T_0$  is 273°K,  $\sigma_k$  is the surface tension between ice and liquid water,  $v_k$  is the specific volume of ice,  $\Delta H_s$  is the specific heat of fusion, and  $d$  is the linear dimension of a cubic crystal. Equation (3) may be used to compute the microcrystal sizes from melting point depression data ( $-30^\circ$  to  $-1^\circ\text{C}$ ) and from the known heat of fusion (231 J/g). The size range of 7 to 200 nm is thus obtained. Assuming the size of the crystals to be identical to the size of the pores, this result is in good agreement with pore size distributions obtained from electron microscopy<sup>3,4</sup> and adsorption measurements.<sup>6,7</sup> As the shape of the melting endotherm is directly related to the distribution of the amount of ice melting, a pore size distribution might be estimated by analyzing the calorimetric results. The shift of the melting peak (see Fig. 3) as a function of increasing water content yields a maximum in the pore size distribution of 22 to 90 nm proportional to the water content. Investigations previously performed by various workers<sup>3,4,6,7</sup> using the same membranes but different experimental techniques have, in sharp contrast, yielded corresponding maxima in pore size distribution of only about 20 nm.

As Kuhn<sup>23</sup> pointed out, this disagreement might be a consequence of crystal growth during the freezing process during which some of the intramolecular bindings between polymer chains might be broken and, in turn, possibly enlarging the pores by mechanical expansion. Consequently, larger pore sizes would result by analysis of the melting endotherms than those originally existing within the polymer matrix.

In summary, the calorimetric data were interpreted by assuming two different states of water in CA membranes. Only bound water without any phase transition was observed in homogeneous membranes. The highly ordered state of water might be due to water-polymer molecule interactions. The calorimetric characteristics of water in homogeneous and asymmetric CA membranes are identical at low water contents ( $v < 16$  wt-%). A reduced heat capacity of water in asymmetric membranes at larger water contents ( $v > 16$  wt-%) coincides with the onset of melting at temperatures below  $0^\circ\text{C}$ . Taking into account the theoretical results of the thermodynamic treatment of capillary phenomena, these experimental findings identify this water of lower heat capacity to be capillary water in the matrix of the asymmetric membranes.

As reported previously, the active layer of asymmetric CA membranes has been proved to contain pores.<sup>5</sup> In addition, it was also suggested that homogeneous CA membranes may contain pores in the range of 10-50 Å.<sup>6</sup> Assuming that the water contained in these pores does not interact with the polymer molecules, this water would be expected to freeze at temperatures in the range of  $-50$  to  $-20^\circ\text{C}$ .<sup>24</sup> Contrary to this expectation, no phase transition of water in homogeneous membranes has been observed. Thus, in connection with the high partial heat

capacity of water found in homogeneous membranes, it might be concluded that the water contained in these small pores interacts with the polymer chains and may thus be present in a more ordered state. Therefore, this kind of "pore" water will not be able to freeze, and thus the calorimetric results reported in this paper may well be consistent with the sorption data.<sup>6</sup> A sorption model describing the water uptake of homogeneous CA membranes over the whole range of water activity without assuming capillary condensation will be discussed in a future paper.

The authors are indebted to Professor R. Schlögl for his interest in this work, to Mr. R. Gröpl for preparing the homogeneous and asymmetric CA membranes, and to Dr. E. Lee for his kind help in preparing the paper. The work was financially supported by the "Bundesminister für Forschung und Technologie," Bonn, Germany.

### References

1. C. E. Reid and E. J. Breton, *J. Appl. Polym. Sci.*, **1**, 1133 (1959).
2. S. Loeb and S. Sourirajan, *Adv. Chem. Ser.*, **38**, 177 (1962).
3. R. L. Riley, J. O. Gardner, and U. Merten, *Science*, **143**, 801 (1964).
4. R. L. Riley, U. Merten, and J. O. Gardner, *Desalination*, **1**, 30 (1966).
5. S. A. Stern, S. K. Sen, and A. K. Rao, *J. Macromol. Sci., Phys.*, **B10**(3), 507 (1974).
6. H.-G. Burghoff and W. Pusch, *J. Appl. Polym. Sci.*, **20**, 789 (1976).
7. H. K. Lonsdale, U. Merten, and R. L. Riley, *J. Appl. Polym. Sci.*, **9**, 1341 (1965).
8. J. L. Williams, H. B. Hopfenberg, and V. Stannett, *J. Macromol. Sci. Phys.*, **B3**, 711 (1969).
9. T. A. Orofino, H. B. Hopfenberg, and V. Stannett, *J. Macromol. Sci. Phys.*, **B3**, 751 (1969).
10. Y. Taniguchi and S. Horigome, *J. Appl. Polym. Sci.*, **19**, 2743 (1975).
11. H. Yasuda, H. G. Olf, B. Crist, C. E. Lamaze, and A. Peterlin, in *Water Structure at the Water Polymer Interface*, H. H. G. Jellinek, Ed., Plenum, New York, 1972, pp. 39-55.
12. M. N. Plooster and S. N. Gittlin, *J. Phys. Chem.*, **75**, 3322 (1975).
13. S. Manjikian, S. Loeb, and J. W. McCutchan, Proc. 1st Int. Desalination Symposium, Paper SWD/12, Washington, D.C., 1965.
14. D'Ans-Lax, *Taschenbuch für Physiker und Chemiker*, Vol. 1, Springer-Verlag, Berlin, 1967.
15. B. Wunderlich and H. Bauer, *Kolloid Z. Z. Polym.*, **241**, 1057 (1970).
16. H. B. Bull and K. Breese, *Arch. Biochem. Biophys.*, **128**, 497 (1968).
17. H.-G. Burghoff, W. Pusch, and E. Staude, Proc. 5th Int. Symposium on Fresh Water from the Sea, Alghero, May 16-20, 1976, Vol. 4, A. and E. Delyannis, Eds., 1976, pp. 143-156, Athens.
18. L. Nicolais, E. Drioli, C. Migliaresi, H.-G. Burghoff, and W. Pusch, *Int. J. Polym. Mater.*, **6**, 175 (1978).
19. A. R. Haly and J. W. Snaith, *Biopolymers*, **6**, 1355 (1968).
20. V. V. Tarasow and G. A. Yunitskii, *Zhur. Fiz. Khim.*, **39**, 2077 (1965).
21. W. A. P. Luck and U. Siemann, private communication.
22. F. Franks, *Water, A Comprehensive Treatise*, Vol. 5, Plenum, New York, 1975.
23. W. Kuhn, *Helv. Chim. Acta*, **39**, 1071 (1956).
24. R. Defay and I. Prigogine, *Surface Tension and Adsorption*, Longmans, London, 1966.
25. R. Schultz and A. Asunmaa, *Rec. Progr. Surface Sci.*, **3**, 293 (1970).
26. R. E. Kesting, *J. Appl. Polym. Sci.*, **17**, 1771 (1973).
27. M. Panar, H. H. Hoehn, and R. R. Hebert, *Macromolecules*, **6**, 777 (1973).

Received July 28, 1977

Revised November 17, 1977